Evolution and Control of 2219 Aluminum Microstructural Features through Electron Beam Freeform Fabrication

Karen M. Taminger[1,a], Robert A. Hafley[1,b] and Marcia S. Domack[1,c]

[1]NASA Langley Research Center, Mail Stop 188A, Hampton, VA 23681 USA

[a]<Karen.M.Taminger@nasa.gov>, [b]<Robert.A.Hafley@nasa.gov>,
[c]<Marcia.S.Domack@nasa.gov>

Abstract. Electron beam freeform fabrication (EBF[3]) is a new layer-additive process that has been developed for near-net shape fabrication of complex structures. EBF[3] uses an electron beam to create a molten pool on the surface of a substrate. Wire is fed into the molten pool and the part translated with respect to the beam to build up a 3-dimensional structure one layer at a time. Unlike many other freeform fabrication processes, the energy coupling of the electron beam is extremely well suited to processing of aluminum alloys.

The layer-additive nature of the EBF[3] process results in a tortuous thermal path producing complex microstructures including: small homogeneous equiaxed grains; dendritic growth contained within larger grains; and/or pervasive dendritic formation in the interpass regions of the deposits. Several process control variables contribute to the formation of these different microstructures, including translation speed, wire feed rate, beam current and accelerating voltage. In electron beam processing, higher accelerating voltages embed the energy deeper below the surface of the substrate. Two EBF[3] systems have been established at NASA Langley, one with a low-voltage (10-30kV) and the other a high-voltage (30-60 kV) electron beam gun. Aluminum alloy 2219 was processed over a range of different variables to explore the design space and correlate the resultant microstructures with the processing parameters. This report is specifically exploring the impact of accelerating voltage. Of particular interest is correlating energy to the resultant material characteristics to determine the potential of achieving microstructural control through precise management of the heat flux and cooling rates during deposition.

Introduction

Electron beam freeform fabrication (EBF[3]) is a new layer-additive process that has been developed at NASA Langley Research Center for near-net shape fabrication of complex structures.[1] EBF[3] uses an electron beam to create a molten pool on the surface of a substrate. Wire is fed into the molten pool and the part translated with respect to the beam to build up a 3-dimensional structure one layer at a time.[1,2,3] Unlike many other freeform fabrication processes, the energy coupling of the electron beam is extremely well suited to processing of aluminum alloys.[4,5]

EBF[3] is a flexible process with many different control variables. Not only can the control variables be used to maintain process consistency, they can also be applied to control attributes within the deposited material. It has already been documented that several process control variables contribute to the formation of these different microstructures, including translation speed, wire feed rate, beam current and accelerating voltage.[1,2,3]

Two EBF[3] systems have been established at NASA Langley. The large EBF[3] system is a modified industrial electron beam welder with a high voltage (30-60 kV) electron beam gun. This system is contained within a 3.8 cm (1.5 in.) thick steel vacuum chamber measuring 2.7 by 2.5 by 1.9 m (108 by 100 by 76 in.). The steel is structurally designed to achieve a 1×10^{-6} torr vacuum level and provide sufficient radiation protection at the higher accelerating voltages. A second EBF[3] system was designed and built for portability with a precision translation system for depositing finer detailed parts. This system uses a lightweight aluminum chamber for enhanced portability, but

provides less radiation protection and therefore is limited to a lower power electron beam gun (10-30 kV) to minimize the level of radiation generated. (X-rays are produced due to the interaction of the electrons with the target substrate. The energy level of those x-rays is a function of the accelerating voltage of the electrons and the atomic number of the substrate material, therefore to minimize the production of x-rays that cannot be absorbed by the vacuum chamber walls, the system must be limited to processing low atomic number materials and/or the accelerating voltage on the electron beam gun be limited below the threshold.) A lower powered gun is also critical to ensuring the portability of the system to minimize the size of the power supply.

Aluminum alloy 2219 has been processed over a range of different processing variables to explore the design space and correlate the resultant microstructures with the processing parameters.[1] Of particular interest is correlating energy to the resultant material characteristics to determine the potential of achieving microstructural control through precise management of the heat flux and cooling rates during deposition. This report will focus specifically on the effects of accelerating voltage on the resulting deposit geometry and microstructure for 2219 aluminum.

Experimental Procedures

The material selected was 2319 aluminum wire, (Al-6 wt%Cu, nominal), which is a weld wire with composition slightly higher in titanium than 2219 to compensate for volitization during the welding (or in this case deposition) process, but otherwise comparable in chemistry, physical and mechanical properties.[6] The total beam power was held constant, while a range of accelerating voltages was examined with the beam amperage adjusted accordingly. Deposits of one, two, and ten layers, 10 cm (4 in.) in length, were made at each of the target accelerating voltage settings of 20, 30, 40 and 50 kV. All deposition runs started with a single pass of beam only (no wire) to clean off any residual oxides and preheat the baseplate to ensure adequate adhesion. The translation speed and mass flow rate were held constant throughout the experiments because it has been documented that both translation speed and mass flow rate of wire into the molten pool will influence the geometry of the deposit and the resulting microstructures.[1] Thus, the only changing variable was the accelerating voltage. Each multiple-layer pass was conducted with a 60-sec. cooling time between deposition of subsequent layers. The deposits were placed 2.5 cm (1 in.) apart to minimize thermal interactions from one deposit to the next. Although this spacing does not eliminate general heating of the baseplate, it is sufficient to prevent overlap of heat affected zones from neighboring deposits.

Due to different wire feed capabilities of the two systems, the 20 kV experiments (performed on the portable EBF^3 equipment) were conducted with 1 mm (0.040 in.) diameter 2319 wire, while the remaining experiments, conducted on the large EBF^3 system, were conducted with 1.6 mm (0.063 in.) diameter 2319 wire. The wire feed rates were adjusted to ensure that the same mass flow rate was attained for each experiment.

After deposition, the specimens were sectioned across the width of the deposits near the center of each linear deposit. This location was selected to eliminate unsteady effects occurring at the beginning and end of each deposit. The cross-sections were mounted, polished, etched, and photomicrographed on an optical metallograph. The depths of penetration, heat affected zones, and width and height of the deposits were measured from the micrographs.

Discussion of Results

Due to the complex thermal history of EBF^3-deposited components, multiple layers were deposited to examine the microstructural evolution during the EBF^3 deposition process. Specimens examined in this study include cross-sections of just the preheat pass, preheat pass plus one, two, and ten layer deposits. The single layer was conducted to measure a baseline depth of penetration and heat affected zone. The two layer deposits were conducted to examine a single interaction layer between

deposits. The ten layer deposits were conducted to examine the impact of accelerating voltage once a steady state condition has been achieved, because as the deposit height increases, the cooling path is reduced to the previous layers, increasing the residual heat until it reaches a constant baseplate temperature. These ten layer deposits were used to compare the height and width of the deposits, the penetration depth, and heat affected zone in the baseplate as a result of the higher heat input from the multiple layers.

Figure 1 shows the microstructure that developed during the preheating pass for a 30 kV sample; this microstructure is representative of all preheating passes observed, regardless of the accelerating voltage. Fine columnar grains nucleate at the base of the molten pool and grow towards the center of the molten pool. The heat affected zone in the baseplate is highlighted by different etching characteristics due to subtle changes in the microstructure.

Figure 1. Representative microstructure for preheat pass only (30 kV accelerating voltage shown).

Figures 2 and 3 show the cross sections of samples after the preheat pass plus a single layer for the 50 kV and 20 kV accelerating voltages respectively. The resulting microstructure from 50 kV (Figure 2) is comparable to the results obtained for 30 kV and 40 kV (not shown). The band at the bottom of the molten pool is a remnant from the preheat pass, with clear definition between the preheat pass and the first deposition layer. For the 20 kV deposit, (Figure 3), the delineation between the preheating pass and the first deposition layer is not as evident. Regardless of accelerating voltage, all single layer deposits had the fine columnar grains at the base of the molten pool observed in the preheat pass. These grains transition to a finely textured dendritic structure at the apex of the deposit, shown in the higher magnification inset.
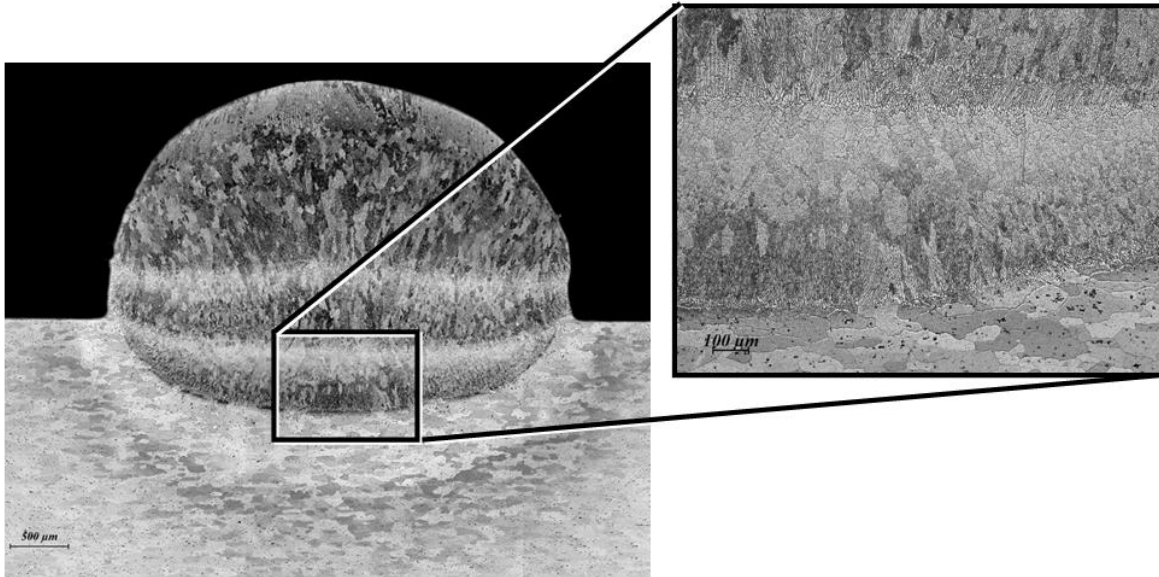

Figure 2. Microstructure of preheat pass plus single layer deposit, representative of 30 to 50 kV deposits (50 kV accelerating voltage shown).
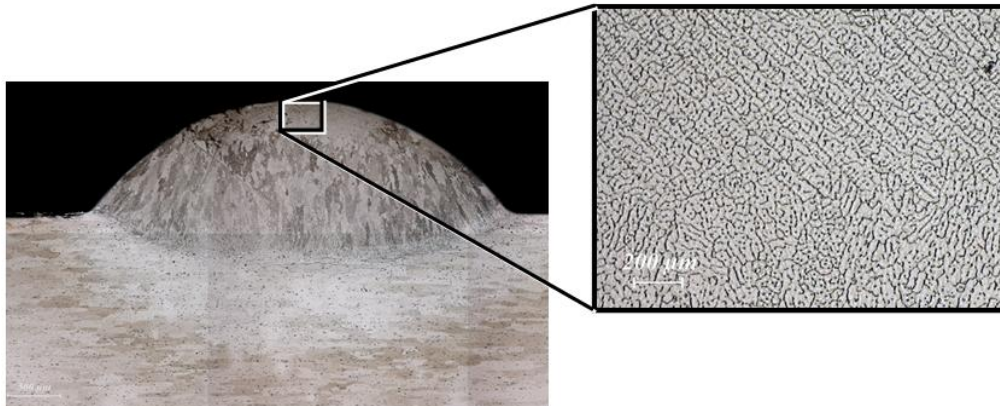
Figure 3. Microstructure of preheat pass plus single layer deposit for 20 kV accelerating voltage.

Figure 4 shows the cross section of a sample after the preheat pass and two layers, made at the 40 kV accelerating voltage. Distinctive light/dark banding is evident in the microstructure between each of the layers. The higher magnification image shows the detail of the banding, where the

dendrites (light colored bands) transition to a columnar grain structure with dendrites growing within the grains, followed by an equiaxed layer that forms at the top of each deposition layer. Note the sharp transition between the equiaxed grains from the top of one layer and the dendtritic grain growth that initiates at the bottom of the molten pool. Specimens fabricated at the other accelerating voltages had similar microstructures, although the banding was less pronounced.


Figure 4. Representative microstructure for preheat pass plus two layers (40 kV accelerating voltage shown).

The cross section of the ten layer deposit at 20 kV (Figure 5) is representative of the ten layer deposits fabricated at the higher accelerating voltages. Comparing the results from the two layer deposit with the lower few layers in the ten layer deposit in Figure 5 provides insight into the microstructural evolution that occurs during the complex thermal history of the EBF^3 process. By the time a ten layer deposit has been built, the lower layers have been repeatedly heated and cooled, until reaching a uniform elevated temperature which facilitates homogenizing the microstructure and enabling mild grain growth to occur. This eliminates the stark banding observed in the two layer deposits such that the differentiation between layers is less pronounced. The fine columnar growth radiating from the bottom of the preheat pass where the deposit meets the baseplate is relatively unaffected, due in part to the larger thermal heat sink of the baseplate and supporting hardware. The banding is much less pronounced in the ten layer deposit, having been homogenized during the thermal cycles produced as subsequent layers were deposited on top of the lower layers. Instead, the grains grow continuously through the deposit layer boundaries in the intermediate region, with finer equiaxed grains in the final (top) layer.

**Figure 5. Microstructure for preheat pass plus 10 layers (20 kV accelerating voltage shown).**

Figure 6 shows the impact of the accelerating voltage on the sizes of the microstructural features measured from the cross-sectioned samples, specifically the width and depth of the heat affected zone within the baseplate and the depth of the molten pool. The depths of the molten pool and the heat affected zone into the baseplate do not significantly change with the number of layers, but do show slightly smaller penetration at the 20 kV accelerating voltage. This phenomenon needs to be examined further to ascertain if this difference is a result of different systems or the lower
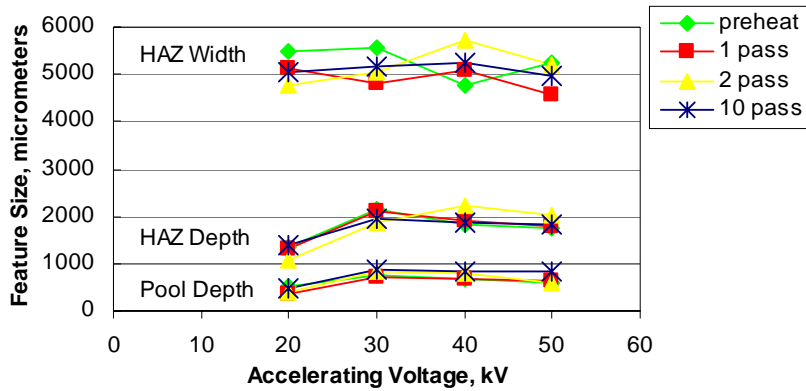
Figure 6. Influence of accelerating voltage on the width and depth of heat affected zone, and depth of molten pool into the baseplate for several different height EBF³ deposits.

accelerating voltage. Note that the depth of the molten pool during the preheat pass is the maximum depth that occurs, regardless of the number of subsequent layers deposited. The molten pool and heat affected zone depths are not changed from the preheating pass to the ten layer deposit. Thus the heat input during the preheating pass is the defining input for the heat affected zone in the baseplate material. This is significant in cases where details are added onto simplified forgings where the thermal input must be controlled to minimize the impact of changes in the microstructures and thus the mechanical properties in the substrate material during the deposition process. The lack of changes in the depth and width of the heat affected zone with increasing number of layers is also interesting because the primary cooling path in the EBF³ process is conduction through the deposit and into the baseplate. The EBF³ process is conducted in a vacuum, so no convection cooling occurs and less than 5% of the heat is dissipated via radiation.

Figure 7 shows the increase in the deposit width with increasing number of layers, as measured at half of the height of the deposit above the surface of the baseplate. The deposit width increases as a result of the molten pool spreading as the heat build-up increases with each subsequent deposited layer. This ultimately reaches a constant width as the temperature within the lower deposit layers become uniform. Although the deposit width is a strong function of the number of layers in the deposit, there is no coupling between the deposit width and the accelerating voltage.
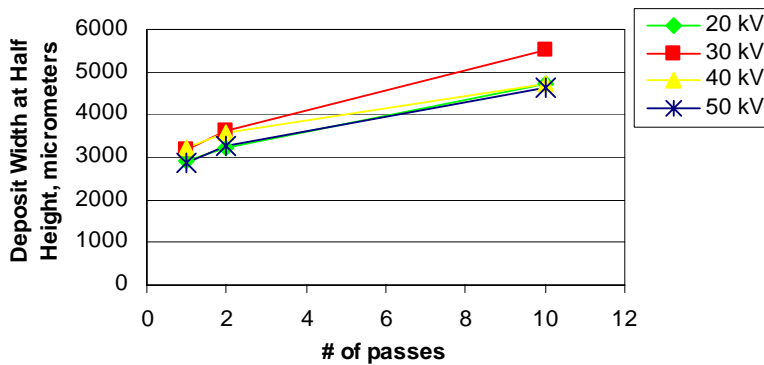
Figure 7. Widths of EBF³ deposits, measured at half the height above the baseplate, increase with increasing deposit heights.

Figure 8 shows the deposit height as a function of the accelerating voltage. These data show that, within the error bars of the sample size, the deposit height is not dependent upon the power used to produce it. The deposit height, therefore, is not coupled to the accelerating voltage used to produce it. These findings for deposit width and height not being a function of the accelerating voltage are consistent with other research.[1,7]
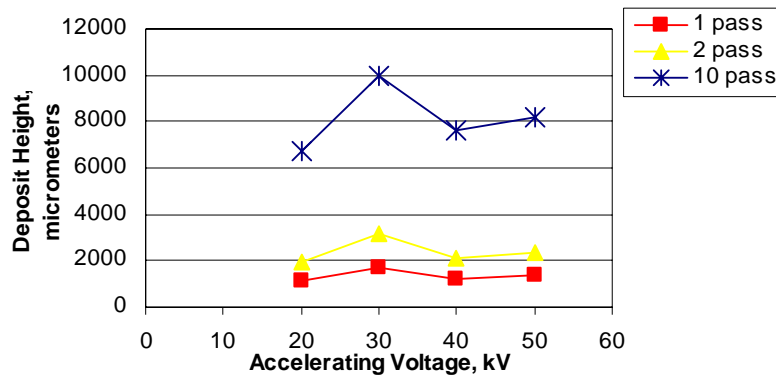
Figure 8. Heights of EBF^3 deposits are not affected by the beam accelerating voltage.

Summary

1. The depth of the molten pool and heat affected zone are similar for accelerating voltages of 30 kV to 50 kV, and slightly lower for 20 kV. This needs to be examined further to ascertain if this difference is a result of different systems or lower accelerating voltage.

2. The molten pool depth into the baseplate and the heat affected zone are not changed from the preheating pass to the ten layer deposit. Thus, the heat input during the preheating pass is the defining input for the heat affected zone in the baseplate material.

3. The width of deposit increases with increasing number of layers due to spreading of molten pool from build up of heat in deposit.

4. The width and height of the deposit are not coupled with the accelerating voltage used.

5. Microstructures evolve during the EBF^3 process. After two layers, banding is clearly evident where the microstructure segregates with distinct regions of dendrites, columnar grains, and equiaxed grains. After ten layers, the banding becomes less obvious, allowing microstructural homogenization and mild grain growth to occur in the lower deposited layers.

References

[1] Taminger, K. M. B., and Hafley, R. A., "Characterization of 2219 Aluminum Produced by Electron Beam Freeform Fabrication," *Proceedings of 13th SFF Symposium*, 482-489 (2002).

[2] Dave, V.R., Matz. J.E., and Eagar, T.W., "Electron Beam Solid Freeform Fabrication of Metal Part," *Proceedings of 6th SFF Symposium*, 64-71 (1995).

[3] Brice, C.A., et al., "Rapid Prototyping and Freeform Fabrication via Electron Beam Welding Deposition," *Proceeding of Welding Conference* (2002).

[4] Jenney, C.L. and O'Brien, A. eds., *Welding Handbook*, Vol. 1, 9th Ed., American Welding Society, 305-306 (2001).

[5] O'Brien, R. L., ed., *Welding Handbook*, 8th Ed., Vol. 2, Ch. 21; American Welding Society, 672-711 (1991).

[6] Mayer, L.W., *Alcoa Green Letter: Alcoa Aluminum Alloy 2219*, (1967).

[7] Wallace, T.A., Bey, K.S., Taminger, K.M.B., and Hafley, R.A., "A Design of Experiments Approach Defining the Relationships Between Processing and Microstructure for Ti-6Al-4V," *Proceedings of 15th SFF Symposium*, (2004).